Human Astrovirus MLB replication *in vitro*: persistence in extra-intestinal cell lines

Diem-Lan Vu[a,b], Albert Bosch[a], Rosa Maria Pintó[a], Enric Ribes[c], Susana Guix[a]

[a] Enteric Virus Laboratory, Department of Genetics, Microbiology and Statistics, University of Barcelona, Barcelona, Spain; Nutrition and Food Safety Research Institute (INSA·UB), University of Barcelona, Barcelona, Spain

[b] Department of Infectious Diseases, Geneva University Hospitals, Switzerland

[c] Enteric Virus Laboratory, Department of Cell Biology, Physiology and Immunology, School of Biology, University of Barcelona, Barcelona, Spain

Running title: Cell culture propagation of MLB astrovirus

Corresponding authors:

Susana Guix

susanaguix@ub.edu

Diem-Lan Vu

diem-lan.vu@ub.edu

Abstract word count: 247

Manuscript word count: 5456

Abstract

MLB astroviruses were identified 10 years ago in feces from children with gastroenteritis of unknown etiology, and have been unexpectedly detected in severe cases of meningitis/encephalitis, febrile illness of unknown etiology and respiratory syndromes. The aim of this study was to establish a cell culture system supporting MLB astrovirus replication. We used two clinical strains to infect several cell lines: a MLB1 strain from a gastroenteritis case, and a MLB2 strain associated with a neurologic infection. Efforts to propagate the viruses in the CaCo-2 cell line were unsuccessful. In contrast, we identified two human non-intestinal cell lines, HuH-7 and A549 cell lines, permissive for both genotypes. After serial passages in the HuH-7.5 cell line, the adapted strains were able to establish persistent infections in HuH-7.5, HuH-7AI and A549 cell lines, with high viral loads (up to 10 $\log_{10}$ genome copies/ml) detected by RT-qPCR in the culture supernatant. Immunofluorescence assays demonstrated infection in about 10% of cells in persistently infected cultures. Electron microscopy revealed particles of 32-33 nm in diameter after negative staining of cell supernatants and capsid arrays in ultrathin sections with a particularly high production in HuH-7.5 cells. IFN expression by infected cells and effect of exogenous IFN varied depending on the type of infection and the cell line. The availability of a cell culture system to propagate MLB astroviruses represents a key step to better understand their replicative cycle, as well as a source of viruses to conduct a wide variety of basic virologic studies.

Importance

MLB astroviruses are emerging viruses infecting humans. More studies are required to determine their exact epidemiology, but several reports have already identified them as the cause of unexpected clinical diseases, including severe neurologic diseases. Our study provides the first description of a cell culture system for the propagation of MLB astroviruses, enabling the study of their replicative cycle. Moreover, we demonstrated the unknown capacity of MLB astrovirus to establish persistent infections in cell culture. Whether these persistent infections are also established *in vivo* still remains unknown, but the clinical consequences would be of high interest if persistence was confirmed *in vivo*. Finally, our analysis of the IFN expression provides some trails to understand the mechanism by which MLB astroviruses can cause persistent infections in the assayed cultures.

Introduction

Firstly identified in 1975 in stool samples of children with diarrhea (1), human astroviruses (HAstVs) cause viral gastroenteritis worldwide (2), being the third most common cause in the pediatric population, after rotavirus and norovirus. Besides children, HAstV gastroenteritis also frequently occurs in the elderly (3) and in immunocompromised individuals (4-6). They are small (28-41 nm in diameter), non-enveloped, single-stranded positive sense RNA viruses. To date, the family *Astroviridae* is divided in two genera: *Mamastrovirus* and *Avastrovirus*, including viruses infecting mammals and birds, respectively. Their genome codes for three open reading frames (ORFs), with ORF1a and ORF1b encoding the protease and polymerase proteins, respectively, and ORF2 the capsid proteins.

With the advent of next-generation sequencing technologies, two novel groups of highly divergent HAstVs (named MLB and VA/HMO) which are more closely related to certain animal astroviruses than to the classic HAstVs have been identified in human stools of individuals with diarrhea (7-13), but also in asymptomatic healthy controls (14, 15). To date, no definitive association between novel astroviruses and gastroenteritis has yet been established, but further epidemiologic studies have confirmed the presence of novel HAstVs worldwide (14, 16-21). In addition, novel HAstVs have been recently identified as the cause of unexpected central nervous system infections in – mostly immunocompromised - humans (22-28). Specifically, MLB astroviruses have been involved in one case of acute meningitis in a healthy young adult (28), and in two cases of neurologic infections in immunocompromised patients (27, 28). Both groups of novel HAstVs have been further divided into several genotypes: MLB1-3 for MLB astroviruses, and VA1-5 for VA astroviruses (2, 29).

Novel HAstVs are part of the neurovirulent astroviruses, which also include animal astroviruses (30). Other unexpected clinical manifestations recently associated with human and animal astroviruses include respiratory tract infections (31-37), fever of unknown etiology (38, 39), hepatitis (40, 41), and severe gout in goose (42). Altogether, these findings suggest that there are probably other still unrecognized divergent astroviruses with clinical implications beyond gastroenteritis, in humans and animals. The potential for cross-species transmission is high (43, 44) and the increasing number of descriptions of non-enteric severe clinical manifestations in animals, especially neurologic involvement, should prompt us to validate appropriate systems to study the pathogenicity of astroviruses. Among the novel human astroviruses, a cell culture system has been recently described for VA1 (45). The present study aims at describing a cell culture system for the propagation of MLB1 and MLB2 astroviruses, the two MLB

genotypes most frequently identified, and providing some clues for understanding their pathogenicity.

Results

MLB astroviruses can be propagated in HuH-7.5 hepatoma cells

Several MLB clinical specimens were used to infect different cell lines and perform serial viral passages (V-P), following a protocol for an acute infection (see Material and methods section). Three MLB1 strains were recovered from stool samples of children under 5 year old with symptoms of acute gastroenteritis and three MLB2 strains were recovered from stool samples and included a neuro-invasive strain identified in an immunocompromised adult patient (28). Among these, only two strains were able to replicate in cell culture (**Figure 1**): one MLB1 strain recovered from a 1-year-old child, and the MLB2 neuro-invasive strain recovered from the 37-year-old immunocompromised patient. Attempts to propagate these strains in CaCo-2 cell line resulted in loss of genome detection after 2 passages (**Figure 2A**). Using HuH-7.5 cells, we observed sustained viral genome detection in the culture supernatant (SN) for up to 8-9 passages, and some viral passages were also successful in A549 cells (**Figures 1A and 2A**). Electron microscopy of the supernatant of acutely infected Huh7.5 cells confirmed the presence of viral capsids of both genotypes, of a mean size of 33±3 nm for MLB1 and 32±2 nm for MLB2 (**Figures 2B and 2C**).

Multi-step growth curves were performed to define infection kinetics (**Figure 3A and B**). While increase of viral RNA in the cellular fraction showed a similar kinetic for both viruses, with a major increase during the first 2 days after inoculation and a total $\log_{10}$ fold increase from 1 hour post-infection (hpi) to 7 days post-infection (dpi) of 3.41±0.37 for MLB1 and 3.22±0.49 for MLB2 (**Figure 3A**), increase of viral RNA in

the supernatant fraction was much higher for MLB2 than for MLB1 (5.14±0.03 vs 2.99±0.20, $p<0.05$) (**Figure 3B**), resulting also in an overall higher viral production for MLB2. We also confirmed the occurrence of infectious viruses in the inoculum by treating it for 5 minutes at 99ºC and confirming the lack of viral RNA increase in the supernatant of infected cultures (data not shown).

A trypsin treatment was initially included, but no significant differences were observed in the efficiency of MLB replication in the presence or absence of trypsin (5 µg/ml) in the post-infection medium (**Figure 3C**).

MLB astroviruses can persistently infect cell cultures

According to the high intracellular viral titer fraction observed for MLB1, we hypothesized that this could reflect a persistent infection. To ascertain whether infected cultures were able to regrow after infection, we used the MLB1 V-P7 cell lysate to establish a persistent infection in HuH-7.5 cell line. Infected cells were trypsinized at 4 dpi and could be further maintained for up to at least 20 cell passages (C-P) (**Figure 1A**). The presence of numerous capsid arrays in persistently-infected HuH-7.5 cells, mostly associated with cell membrane vesicles, was observed (**Figure 4**). Cells containing capsid arrays showed remarkable cell structure reorganizations.

To elucidate if this was due to the described defect in the interferon pathway of HuH-7.5 cell line (46, 47), we similarly initiated a persistent infection on HuH-7AI cells with both HAstV MLB1 and MLB2 strains recovered from cell lysates, and also on A549 cells, according to the supposed respiratory tropism of novel astroviruses (**Figure 1B**). Titers of viral genomes for both strains detected in the supernatant of the two cell lines during passages of persistently infected cultures are shown in **Figure 5A**. The mean

viral titer for MLB1 was significantly higher than MLB2 in HuH-7AI and A549 cell lines ($p<0.002$; **Figure 5B**). MLB1 mean viral titer was also significantly higher in HuH-7.5 cells compared to HuH-7AI cells, which could confirm our initial hypothesis that the HuH-7.5 interferon pathway deficiency could promote MLB1 replication ($p<0.001$; **Figure 5A**).

Attempts to establish a MLB2 persistent infection on HuH-7.5 cell line were however unsuccessful, and we decided to pursue the rest of the experiments on HuH-7AI and A549 cells only, in order to be able to compare the results between both genotypes. Except at 4 days after C-P0, persistently infected cultures did not show cytopathic effect, and cells were morphologically identical to non-infected cells. Of note, attempts to establish a persistent infection on CaCo-2 cells showed a progressive decline of the viral titer from one cell passage to another, reason why we did not pursue with this cell culture system neither (**Figure 5A**).

Indirect immunofluorescence assays confirmed the presence of viral capsid proteins in infected cells. **Figure 6A** shows capsid protein formation in each cell line persistently infected by MLB1 and MLB2 strains. While the fluorescent intensity in each cell line reflects a high production of capsid protein in infected cells, the proportion of cells showing capsid proteins ranged between 1-18% (median 11% and 4.8% for HuH-7AI and A549 persistently infected with MLB1, respectively, and 8.8% for both cell lines persistently infected with MLB2) (**Figure 6B**). Overall, for HAstV MLB1, the percentage of capsid-expressing cells was significantly higher in HuH-7AI cells than in A549 cells. No differences were observed for HAstV MLB2. Electron microscopy also confirmed the presence of viral capsid arrays within HuH-7AI and A549 infected cells (**Figure 7**). **Table 1** summarizes the results of HAstV MLB1 and MLB2 propagation on selected cell lines.

Complete genome sequences, using primers detailed in **Table 2**, were obtained for both strains to analyze whether mutations were occurring during replication compared to viral sequences present in the clinical specimens. The nucleotide sequences of wild-type strains recovered from clinical samples are available at Genbank (accession numbers MK089434 and MK089435). For MLB1, sequences were obtained at V-P6 and C-P2 of acute and persistent HuH-7.5 cell infections, respectively. For MLB2, sequences were obtained at V-P2 on A549 cells and V-P3 in HuH-7.5 cells. No nucleotide changes were detected on the whole genomes throughout the analyzed passages. Nevertheless, we could observe a A/C polymorphism at position 1313 and a C/T polymorphism at position 5477 of MLB2 at V-P2 in A549 cells, probably reflecting the presence of virus quasiespecies. While this latter mutation would be synonymous (and was also present in the wild-type strain), mutation at position 1313 would result in a substitution of a Lysine (K) residue by an Arginine (N) in ORF1a. Interestingly, HAstV MLB1 strain directly recovered from the stool sample was also able to establish a persistent infection in HuH-7.5 cell line, with viral titers comparable to the persistent infection with HAstV MLB1-adapted strain (**Figure 5A**), confirming that the ability to establish persistent infections in cell cultures is not dependent on any specific adaptative mutation.

Lack of a strong type I interferon response in MLB-infected cultures

We measured the expression of IFN-β and IFN-λ1, both known to be implicated in the antiviral innate response. PolyI:C transfection was used as a positive control of IFN induction and GAPDH mRNA levels were used for normalization. During the acute infection, we could not detect any expression of IFN-λ1, and only a low expression of IFN-β mRNA from 4 to 7 dpi in A549 cells infected with MLB1 and MLB2, compared to polyI:C control (**Figure 8A**). In order to confirm that the absence of IFN expression in HuH-7AI was not due to the fact that only a small proportion of these cells were

infected, we infected them with the highest multiplicity of infection possible according to the viral titer of the stocks (MOI 25,000 genome copies/cell for MLB1 and 680 genome copies/cell for MLB2), which resulted in the infection of >80% of HuH-7AI cells (as visualized by immunofluorescence, **Figure 8B and 8C**), and IFN mRNA remained undetectable. During persistent infections, there was basically no expression of IFN-β nor IFN-λ1 mRNAs, in any of the two cell lines, infected with MLB1 or MLB2 (**Figure 8D**).

To understand whether MLB1 and MLB2 replication could block type I IFN expression induced by dsRNA, we analyzed IFN-β and IFN-λ1 mRNA expression after transfecting polyI:C in persistently-infected cultures. We could observe that IFN-β and IFN-λ1 mRNA expression was almost undetectable in A549 cells for both genotypes compared to positive control, while in HuH-7AI cell line, IFN-β and IFN-λ1 induction was only blocked by MLB2. MLB1 genotype slightly inhibited the expression of IFN-λ1 but not of IFN-β (**Figure 8D**). The possibility that A549 persistently infected cultures were refractory to transfection was ruled out by confirming that cells could be efficiently transfected using a green fluorescent protein (GFP)-encoding plasmid (data not shown). Altogether, these results suggest that MLB replication is able to disrupt the innate immune sensing pathway induced by polyI:C, although this behavior is cell and genotype (or strain)-dependent.

Exogenous IFN inhibits viral replication in a cell-dependent manner

Finally, we tested if the addition of exogenous IFN-β1a and IFN-λ1 at 1,000 U/ml could inhibit viral replication when acutely infected, and cure the persistently-infected cell lines. During acute infection, pre-treatment of cells with both IFN-β1a and IFN-λ1 resulted in a statistically significant reduction in the viral titer, compared to mock-treated controls ($p<0.005$ and $p<0.01$ for IFN-β1a and IFN-λ1, respectively, during

MLB1 infection of both cell lines; $p<0.001$ and $p<0.005$ for IFN-β1a and IFN-λ1, respectively, during MLB2 infection of both cell lines; **Figure 9A and 9B**). The inhibitory effect of both IFNs were higher in HuH-7AI cells compared to A549 cells ($p=0.02$). For both genotypes and in both cell lines, the effect of IFN-β1a was approximately two-fold higher compared to IFN-λ1 (average $\log_{10}$ reductions of 2.91±0.11 versus 1.59±0.11 for MLB1 in HuH-7AI, 1.92±0.52 versus 0.94±0.11 for MLB1 in A549; 4.35±0.03 versus 2.30±0.25 for MLB2 in HuH-7AI; and 2.64±0.20 versus 1.33±0.02 for MLB2 in A549).

During persistent infection, the addition of IFN-β1a to the culture media succeeded in curing the HuH-7AI cell culture from both MLB1 and MLB2 persistent infection after several cell passages. Addition of IFN-λ1 did not eliminate viral replication completely, but reduced viral titer 0.96±0.21 and 2.37±0.09 $\log_{10}$ for MLB1 and MLB2, respectively, after 7 passages (**Figure 9C and 9D**). In opposite, in the A549 persistently-infected cell cultures, addition of none of the tested IFNs produced an inhibitory effect on viral replication (**Figure 9E and 9F**). Increase of IFN concentration up to 5,000 U/ml for two additional passages had no effect either (data not shown).

Discussion

We provide the first description of several cell culture systems permissive for the novel HAstV MLB replication. Both HuH-7 and A549 cell lines were infected by viruses present in clinical specimens and sustained viral replication during serial cell passages without addition of viral inoculum. Expressed viral capsid protein was detected by immunofluorescence within persistently infected cultures and viral capsids were

visualized by electron microscopy both within membrane vesicles and in the cell cytosol. The production of infectious virions released into the supernatant of persistently infected cultures was confirmed by their ability to acutely infect naïve cells when used as inoculum, and generate virions that could be observed in the cell culture media after negative staining. In addition, we provide data on replication of two distinct genotypes, allowing to compare the behaviors of HAstV MLB1 and MLB2. Nevertheless, we cannot exclude that the results could be strain-dependant, as we only succeeded in propagating one strain of each genotype.

We found that the addition of exogenous trypsin is not required for efficient replication of MLB strains, as previously described for VA1 strains by Janowski *et al* (45). The efficient propagation of HAstV MLB in extra-intestinal cell lines, hepatic and respiratory, reinforces this information, as these tissues do not secrete as much trypsin as the intestinal tract (48). The capacity of novel HAstVs to infect tissues without the need for capsid activation by trypsin opens the door to a potential wider tissue tropism i*n vivo*, which could explain the diverse clinical manifestations that have been recently described with divergent astrovirus strains: acute hepatitis, respiratory illnesses, gout, or encephalitis. Nevertheless, our attempts to infect CaCo-2 cells were unsuccessful (or at least not as efficient as with HuH-7 and A549 cells, according to the persistent infection assays), which distinguish our results from those of Janowski *et al* and those on classical astroviruses. Whether this difference is strain-dependent cannot be formally ruled out, but the hypothesis that divergent astroviruses could show an exclusively extra-intestinal tropism has also been advanced by other groups (49), who found porcine astrovirus genome in the central nervous system, respiratory tract and circulatory system of pigs affected by a neurologic syndrome, but not in stool samples. Their work suggests that the respiratory tract could be the primary site of astrovirus infection,

before spreading to the central nervous system. Of note, classical and VA1 astroviruses are also able to infect A549 cells (45, 50).

Apart from providing a cell culture system for HAstV MLB propagation, we have identified the capacity of this clade to establish persistent infection in the studied continuous cell lines. To the best of our knowledge, this is the first description of an experimentally proven persistent infection for astroviruses. RNA viruses make use of several mechanisms for persistence – including the innate immune system evasion - and most of persistent infections are asymptomatic (51, 52). Thereby, although continuous cell lines are not the best model to infer issues related to pathology occurring *in vivo*, it would be very interesting to further study if there is any role for persistent infection in astrovirus diseases, and if so, which are the determinants for the virus to switch from persistence to virulence. Our immunofluorescence assay and structural changes observed by electron microscopy indicate a carrier-state infection, characterized by a few proportion of capsid-expressing cells, associated with a high degree of cell damage and a high production of virus progeny (53) that can infect surrounding non-infected cells. This model of infection is well described for group B coxsackie viruses (54, 55). An alternate hypothesis is that most of cells in the culture may be resistant to a full cycle of viral replication – precluding to capsid visualization by immunofluorescence - and continue to divide. In light of the impossibility to establish a MLB2 persistent infection in HuH-7.5 cells, it seems that the high rate of replication of MLB2 genotype during the acute infection prevents the survival and regrowth of the infected cells after subculture.

The results of our IFN experiments provide clues to understand the mechanism for HAstV MLB persistence, suggesting that MLB infection does not induce an early strong IFN expression, as it has already been described for the classical HAstVs (56). This

would avoid a complete clearance of infection by cells and enable persistence. The fact that no IFN expression was observed in any acutely infected cell line before 4 dpi, the time point when infected cultures were subcultivated from C-P0 to study persistence, supports this idea, permitting the virus to continue replicating in permissive cells before the intervention of the innate immune response. Only a certain level of IFN-β mRNA expression was detected in A549 cells during the late course of acute infection. The inhibition of HAstV MLBs replication with exogenous IFN during acute infection also reinforces these data: if there was no shut down of IFN expression, efficient production of IFN by infected cells would inhibit viral replication and thus possibly prevent persistent infections. Of note, sensitivity of astroviruses to IFN when cells are pre-treated before infection has also been demonstrated for classical HAstV (56, 57) and VA1 astroviruses (45).

Exogenous IFNs, especially IFN-β1a, were also able to inhibit and even eliminate MLB viruses from persistently infected cultures, but this was only observed for HuH-7AI cells and not for A549 cells. While this difference based on cell type was unexpected, it suggests that persistence may be maintained in both cell lines by dissimilar mechanisms. Indeed, the inhibitory effects of both IFNs on A549 cells were also significantly milder than on HuH-7AI when cells were acutely infected. It is also noteworthy that the effect of MLBs replication on IFN mRNA expression induced by polyI:C transfection was different in both cell lines. While it could be efficiently blocked on A549 cells, this effect was only partial in HuH7-AI. Our hypothesis is that while MLBs cannot inhibit IFN expression induced by polyI:C, they may still avoid activation of IFN response by an unknown mechanism, allowing their persistence in the culture unless IFN is added exogenously. On A549 cells, however, MLBs may find the mechanisms to inhibit both arms of the IFN response (induction and action), allowing

316 them to persist in the culture. The fact that efficient counteracting IFN action on A549
317 cells is only observed when cells are already infected and not when they are acutely
318 infected suggests that a factor expressed at late stages of the replication cycle may be
319 required.

320 Whether our inability to establish a persistent infection on HuH-7.5 cell line with the
321 MLB2 strain was due to the activation of other cellular innate responses that would
322 induce expression of antiviral genes in non-infected neighboring cells or whether it was
323 due to technical factors such as the schedule of culture passaging or to the MOI remains
324 to be elucidated. In addition, we did not measure other types of IFN such as IFN-α,
325 which could also play a role in the course of HAstV infection. Altogether, we can see a
326 distinct IFN expression and response to exogenous IFN between the persistent versus
327 acute infection, between MLB1 and MLB2 and between different cell lines. These
328 results suggest that there is an actual co-evolution between a virus and its host and that
329 many factors (virus strain, cell type, model of infection) may uniquely influence the
330 course of the infection. Interestingly, Nice *et al.* recently demonstrated that IFN-λ was
331 able to reduce and to cure persistent infection of murine norovirus in the absence of an
332 adaptive immune response (58, 59), and that the interaction between host IFN-λ
333 response and some viral nonstructural proteins determined viral tropism (59). In
334 addition, these results also suggest that, if persistence was confirmed *in vivo*, in case of
335 co-infections, certain MLB HAstVs could potentially promote the replication of other
336 viruses by inhibiting IFN response.

337 In summary, we provide a cell culture system for the propagation of the novel HAstV
338 MLB. We have demonstrated that these viruses can establish a carrier-state infection *in*
339 *vitro* on extra-intestinal human cell lines. IFN expression may be altered by HAstV
340 MLB infections although may vary depending on the strain, the cell line and the model

of infection. Finally, HAstV MLB sensitivity to IFN also depends on the type of infection, the genotype, the cell line and the type of IFN.

Materials and Methods

Cell lines

Human epithelial colorectal adenocarcinoma (CaCo-2 cells; ECACC 86010202), human hepatocyte-derived cellular carcinoma (HuH-7AI cells (60) and HuH-7.5 cells (61)) and adenocarcinoma human alveolar basal epithelial (A549 cells; ATCC-CCL 185) cell lines were grown at 37°C with 5% $C0_2$, on MEM with L-glutamine supplemented with 10% of fetal bovine serum (FBS; Gibco) and 100 units/mL of penicillin and streptomycin (Gibco).

Clinical specimens

Stool samples positive for MLB1 were collected during a screening of stool samples in children under 5 years old with acute gastroenteritis in Barcelona, Spain. Stool samples positive for MLB2 were identified in a previous study (28). Three samples positive for MLB1 and three samples positive for MLB2 were used for infection, with a viral titer ranging from $1.5x10^6$-$1.2x10^8$ genome copies/ml of inoculum for MLB1 and from $2.8x10^4$-$4.6x10^7$ genome copies/ml of inoculum for MLB2.

Acute infections

Stool suspensions of 0.1 g of stool sample diluted in 900 µl of PBS were filtered through a 0.45 µm filter (Millipore) and then diluted 1:2 with MEM 0% FBS, and were used as initial inoculum. The inoculum was pretreated with trypsin (Gibco), at a final concentration of 10 µg/ml, at 37°C for 30 minutes. Cells were grown on a 24-well plate

364 to 80-100% confluency and washed twice with MEM 0% FBS before infection with 200
365 µl of the stool inoculum diluted 1:2 after trypsin pretreatment. Cells were incubated for
366 one hour at 37°C and the inoculum was then removed and replaced by 500 µl of MEM
367 0% FBS supplemented with 0.03% kanamycin, penicillin and streptomycin, and 5µg/ml
368 trypsin. Cells were maintained at 37°C and 5% CO_2 for 7 days and the medium was
369 changed every other day. After 7 days, cells were freezed/thawed three times and 100 µl
370 of the cell lysate was used for the next viral passage. Subsequent viral passages (V-P) as
371 acute infections were performed without trypsin pre-treatment and with addition of
372 MEM supplemented with 10% FBS without trypsin in the post-infection media.

373 **Persistent infections**

374 A cell lysate of the viral passage 7 (V-P7) of the acute viral passages on HuH-7.5 cells
375 was used to persistently infect the HuH-7AI, A549 and CaCo-2 cell lines with MLB1
376 and MLB2, respectively (**Figure 1B**). The viral titer in these selected cell lysates was
377 determined as viral genome copies/ml by RTqPCR assay, and as infectious viruses/ml
378 by $TCID_{50}$ assay in HuH-7.5 cells. Briefly, for $TCID_{50}$ assay, cells were infected with
379 10-fold serial dilutions of each sample in quadruplicate, as described above for acute
380 infections. After 7 days, nucleic acids were extracted from 50 µl of supernatant from
381 each well and a RT-qPCR assay was performed for the detection of viral genomes (see
382 below). The $TCID_{50}$ was calculated using the Spearman-Karber method, with any
383 detection of viral genome in a well being considered as infected. 1 $TCID_{50}$ corresponded
384 approximately to $1.4x10^4$ genomes for MLB1 and to $1.5x10^3$ for MLB2. A multiplicity
385 of infection (MOI) of approximately 1,000 genome copies per cell (0.07 infectious
386 viruses per cell) and 20 genome copies per cell (0.01 infectious viruses per cell) was
387 used for MLB1 and MLB2, respectively. For the first passage, cells were grown on 24-
388 well plates to 80-100% confluency and washed twice with MEM 0% FBS. Cell lysates

were diluted in MEM 0% FBS to a final volume of 200 µl at the desired MOI and was inoculated to the cells. After 1-hour incubation at 37°C, the inoculum was removed and replaced by 500 µl of MEM 10% FBS. There was no pretreatment or addition of trypsin for the persistent infections. Cells were incubated at 37°C for 4 days before being subcultivated by trypsinization at a split ratio 1:3 for a subsequent passage. Cells were then subcultivated by trypsinization for serial passages without addition of viral inoculum. Persistently infected cells were maintained in T75 flasks, and subcultivated every 7-10 days at a split ratio 1:3-1:6. An aliquot of the supernatant before each subculture was collected to monitor viral titer.

Viral RNA extraction and quantitative reverse-transcription polymerase chain reaction (RT-qPCR) assay

RNA was extracted from the cell culture supernatants using the NucleoSpin® RNA virus kit (Macherey-Nagel) following the manufacturer's instruction, and RT-qPCR specific assays for MLB astroviruses were performed as previously published (19). Briefly, the following primers and probe for MLB1 were used: forward primer 4320: 5'-GGTCTTGGAGCYCGAATTC-3'; reverse primer 4387: 5' CGCTGTTTAATGCGCCAAA 3'; hydrolysis probe 4349: 5' [FAM] TAGRGTTGGTTCAAATCT [MGBNFQ] 3'. The primers and probe used for MLB2 were as follows: forward primer 3762: 5' CCGAGCTCTTAGTGATGCTAGCT 3'; reverse primer 3832: 5' CACCCCTCCAAATGTACTCCAA 3'; hydrolysis probe 3793: 5' [VIC] CGCTTCACTCGGAGAC [MGBNFQ] 3'. Plasmids containing a 125 bp-fragment of the MLB1 (spanning nucleotides 4292-4416 from FJ222451) and MLB2 (spanning nucleotides 3724-3848 from KT224358) genomes were used as controls for quantification, and RT-qPCR was performed using the Kapa Probe Fast Universal One-Step RT-qPCR Master Mix (Kapa Biosystems) following the manufacturer's

instructions, on a CFX96 Touch™ Real-Time PCR Detection System (Bio-Rad). 15 µl of the RT-qPCR master mix were mixed with 5 µl of extracted RNA. The reaction conditions were as follows: 42°C for 15 minutes, 95°C for 5 minutes, then 40 cycles of 95°C for 3 seconds, 55°C for 20 seconds, 72°C for 10 seconds. Standard curves were constructed based on 10-fold serial dilutions of the corresponding MLB plasmid analyzed in duplicate.

Multistep growth curve

The multistep growth curve was performed using a MOI of 20 genome copies/cell for both MLB1 and MLB2. Infection was performed on 24-well plates according to the protocol used for acute infection (without the use of trypsin nor the change of medium every other day). At each indicated time point, 50µl of the supernatant as well as the total cells were collected. RNA extraction of the supernatant was performed using the NucleoSpin® RNA virus kit (Macherey-Nagel) following the manufacturer's instruction, and RNA extraction from cells was performed using the GenElute Mammalian Total RNA Miniprep Kit (Sigma Aldrich), as indicated by the manufacturer's instruction. RT-qPCR assay was performed as described above. Samples were quantified in triplicate from one single experiment.

Immunofluorescence

Indirect immunofluorescence assays were performed using rabbit polyclonal MLB1 capsid peptide (DW60) and MLB2 capsid peptide (DW58) antibodies (kindly provided by Dr David Wang, Washington University School of Medicine) (62) as primary antibodies, and secondary antibodies labeled with Alexa 488. DAPI staining was used to detect nuclei. Briefly, cells were rinsed twice with PBS and fixed with 3% paraformaldehyde in PBS for 15 minutes (min) at room temperature (RT).

Permeabilization was performed for 10 min at RT with 0.5% Triton X-100 in 20mM glycine-PBS. Cells were then blocked for 60 min at RT in 20mM glycine-PBS containing 10% bovine serum albumin, before incubation with primary antibodies with a 1:1000 dilution during 60 min at 37°, and then with the secondary antibodies with a 1:500 dilution during other 60 min at 37°. Incubation with 1µg/ml DAPI (4',6'-diamidino-2-phenylindole) staining was finally performed for 15 min at RT. Cells were washed twice after each step described, except between the blocking step and the incubation with primary antibodies and were kept in PBS at 4° until visualization. Negative controls included cells incubated with pre-immune sera, primary or secondary antibodies alone, and fixed cells alone (sample auto-immunofluorescence). Nuclei and viral capsids were visualized under a Leica DMIRB/MZFLIII fluorescence microscope.

Electron microscopy

Cell culture supernatants were analyzed by transmission electron microscopy after negative staining. A 10-µl sample was applied to a carboncoated 400-mesh copper grid and was stained with 2% phosphotungstic acid at pH 6.4. The grids were examined under a JEOL 1200 electron microscope.

For ultrathin sections, persistently infected cells and non-infected controls were seeded on a 90 mm sterile dish for cell culture until reaching 80-90% confluency. After removing the medium, cells were fixed with 2.5% glutaraldehyde in 0.1 M phosphate buffer (PB) during 60 minutes. Cells were then scrapped in 1.5 ml of PB and collected. After 10 minutes centrifugation at 1000 *g*, the pellet was suspended in PB and washed in agitation at 4°C during 10 minutes (x4). Cells were then post-fixed with 1% osmium tetroxide, 0.8% potassium hexacyanoferrate in 0.1 M PB for 1-2 hours at 4°C. After extensive washing with *Mili-Q* water, sample dehydratation was performed with a graded series of acetone (50% to 100%) and blocs were prepared in Eponate 12.

463 Sections of 55 nm were cut with a Leica UC6 ultramicrotome (Leica Microsystems
464 Inc.). Observation was performed under a JEOL 1200 electron microscope.

465 **Sequence analysis**

466 Primers pairs were designed to amplify ten overlapping amplicons covering the
467 complete genomes (**Table 2**). Reverse transcription was performed using the
468 Superscript IV Reverse Trancriptase (Invitrogen) and cDNA amplification was
469 performed using the Pwo DNA polymerase (Roche), at the following reaction
470 conditions: 70°C for 7 minutes, 50°C for 25 minutes, 80°C for 10 minutes; 94°C for 4
471 minutes, then 40 cycles of 94°C for 30 seconds, 50-55°C for 40 seconds, 72°C for 2.15
472 minutes, and 72°C for 10 minutes. Amplicons were purified by gel electrophoresis and
473 Sanger sequenced with the ABI PRISM BigDye® Terminator Cycle Sequencing Ready
474 Reaction Kit V3.1on an ABI Prism 3700 automatic sequencer (Applied Biosystems).
475 Complete genome sequences for the MLB1 strain obtained from the stool specimen was
476 deposited in Genbank (Accession numbers MK089434 and MK089435).

477 **IFN expression analysis**

478 Intracellular RNA was extracted using the GenElute Mammalian Total RNA Miniprep
479 Kit (Sigma Aldrich), as indicated by the manufacturer's instruction. The resulting
480 eluate was treated with RQ1 RNAse-free DNase (Promega) to remove any trace of
481 genomic DNA. Quantitative reverse-transcription polymerase chain reaction (RT-
482 qPCR) was performed using the manufacturer's instructions for KiCqStart One-step
483 Probe RT-qPCR assay targeting mRNA of GAPDH, IFN-β and IFN-λ1 on a CFX96
484 Touch™ Real-Time PCR Detection System (Bio-Rad). Primers and probes sequences
485 were as follows: GAPDH forward primer: 5'-GAAGGAAATGAATGGGCAGC-3',
486 GAPDH reverse primer: 5'-TCTAGGAAAAGCATCACCCG-3', GAPDH probe: 5'-

[6FAM]ACTAACCCTGCGCTCCTGCCTCGAT[OQA]-3'; IFN-β forward primer: 5'-CCTCCGAAACTGAAGATC-3', IFN- β reverse primer: 5'-GCAGTACATTAGCCATCA-3', IFN- β probe: 5'-[FAM]TAGCCTGTGCCTCTGGGACT[BHQ]-3'; IFN-λ1 forward primer: 5'-CCACCACAACTGGGAAGG-3' IFN-λ1 reverse primer: 5'-TTGAGTGACTCTTCCAAGGC-3' IFN-λ1 probe: 5'-[FAM]AGCGAGCTTCAAGAAGGCCAGGGAC[OQA]-3'. 15 µl of the RT-qPCR master mix were mixed with 5 µl of extracted RNA. The reaction conditions included: 50°C for 20 minutes, 95°C for 1 minute, then 40 cycles of 95°C for 5 seconds and 60°C for 35 seconds. GAPDH mRNA titers were used as an endogenous control to normalize all samples versus the number of cells. All samples were quantified at least in duplicate from two distinct experiments. Positive controls were determined by the transfection of the synthetic analog of dsRNA polyinosine-polycytidylic acid (polyI:C) (InvivoGen) at 1mg/ml on each cell line, using the X-treme HD Roche transfection reagent (Roche) and Optimem Medium (Gibco). Determination by RT-qPCR assay of the IFN expression 24 hours after transfection was then performed as described above. To define a standard curve, 10-fold serial dilutions of the GAPDH, IFN-β and IFN-λ1 RNA were analyzed for each cell line transfected with polyI:C.

Inhibition of MLB HAstV replication with addition of exogenous IFN

We used human IFN-β1a and IFN-λ1 (PBL Assay Science). For the acute infection, cells were grown on a 24-well plate and were pretreated with IFN-β1a or IFN-λ1 at a concentration of 1,000 U/ml for 24 hours before infection. Cells were inoculated with MLB1 and MLB2 at a MOI of 20 genome copies/cell as described before (without the use of trypsin). IFN-β1a or IFN-λ1 were added in the post-infection medium at a

concentration of 1,000 U/ml. 50 µl aliquots were collected from the supernatant at 4dpi for RNA extraction and RT-qPCR (see above).

For persistent infection, persistently-infected cell cultures were subcultured as described before. IFN-β1a or IFN-λ1 were added in the medium post-seeding at a concentration of 1,000 U/ml. 50 µl of supernatant was collected before the next subculture, between 4 and 6 days post-seeding, and viral RNA was extracted and analyzed by RT-qPCR as described before. All passages were performed in duplicate.

Statistical analyses

The Mann-Whitney and ANOVA tests, with additional test of Scheffe when appropriate, were used to compare continuous variables. $P<0.05$ was considered statistically significant. Statistics were performed by Stata /IC 13.1 (StataCorp, College Station, TX, USA).

Acknowledgments

We would like to thank Laurent Kaiser and Samuel Cordey from Geneva University Hospitals, Switzerland, for providing the clinical stool specimens positive for MLB2 and the RT-qPCR assay sequence primers, probes and plasmid controls. We are also grateful to David Wang from Washington University School of Medicine, US, for providing the MLB specific antibodies.

Funding

This work was supported in part by grant 2017-SGR-244 of the Agència de Gestió d'Ajuts Universitaris i de Recerca, and the Biotechnology Reference Network (XRB) program of the Generalitat de Catalunya. Diem-Lan Vu was recipient of a fellowship from Geneva University Hospitals.

534

References

1. Appleton H, Higgins PG. 1975. Letter: Viruses and gastroenteritis in infants. Lancet 1:1297.
2. Bosch A, Pinto RM, Guix S. 2014. Human astroviruses. Clin Microbiol Rev 27:1048-1074.
3. Jarchow-Macdonald AA, Halley S, Chandler D, Gunson R, Shepherd SJ, Parcell BJ. 2015. First report of an astrovirus type 5 gastroenteritis outbreak in a residential elderly care home identified by sequencing. J Clin Virol 73:115-119.
4. Daniel-Wayman S, Fahle G, Palmore T, Green KY, Prevots DR. 2018. Norovirus, astrovirus, and sapovirus among immunocompromised patients at a tertiary care research hospital. Diagn Microbiol Infect Dis 92:143-146.
5. Gallimore CI, Taylor C, Gennery AR, Cant AJ, Galloway A, Lewis D, Gray JJ. 2005. Use of a heminested reverse transcriptase PCR assay for detection of astrovirus in environmental swabs from an outbreak of gastroenteritis in a pediatric primary immunodeficiency unit. J Clin Microbiol 43:3890-3894.
6. Cubitt WD, Mitchell DK, Carter MJ, Willcocks MM, Holzel H. 1999. Application of electronmicroscopy, enzyme immunoassay, and RT-PCR to monitor an outbreak of astrovirus type 1 in a paediatric bone marrow transplant unit. J Med Virol 57:313-321.
7. Finkbeiner SR, Holtz LR, Jiang Y, Rajendran P, Franz CJ, Zhao G, Kang G, Wang D. 2009. Human stool contains a previously unrecognized diversity of novel astroviruses. Virol J 6:161.
8. Phan TG, Nordgren J, Ouermi D, Simpore J, Nitiema LW, Deng X, Delwart E. 2014. New astrovirus in human feces from Burkina Faso. J Clin Virol 60:161-164.
9. Medici MC, Tummolo F, Calderaro A, Elia G, Banyai K, De Conto F, Arcangeletti MC, Chezzi C, Buonavoglia C, Martella V. 2014. MLB1 astrovirus in children with gastroenteritis, Italy. Emerg Infect Dis 20:169-170.
10. Mitui MT, Bozdayi G, Matsumoto T, Dalgic B, Nishizono A, Ahmed K. 2013. Complete Genome Sequence of an MLB2 Astrovirus from a Turkish Child with Diarrhea. Genome Announc 1.
11. Finkbeiner SR, Allred AF, Tarr PI, Klein EJ, Kirkwood CD, Wang D. 2008. Metagenomic analysis of human diarrhea: viral detection and discovery. PLoS Pathog 4:e1000011.
12. Finkbeiner SR, Li Y, Ruone S, Conrardy C, Gregoricus N, Toney D, Virgin HW, Anderson LJ, Vinje J, Wang D, Tong S. 2009. Identification of a novel astrovirus (astrovirus VA1) associated with an outbreak of acute gastroenteritis. J Virol 83:10836-10839.
13. Kapoor A, Li L, Victoria J, Oderinde B, Mason C, Pandey P, Zaidi SZ, Delwart E. 2009. Multiple novel astrovirus species in human stool. J Gen Virol 90:2965-2972.
14. Meyer CT, Bauer IK, Antonio M, Adeyemi M, Saha D, Oundo JO, Ochieng JB, Omore R, Stine OC, Wang D, Holtz LR. 2015. Prevalence of classic, MLB-clade and VA-clade Astroviruses in Kenya and The Gambia. Virol J 12:78.
15. Holtz LR, Bauer IK, Rajendran P, Kang G, Wang D. 2011. Astrovirus MLB1 is not associated with diarrhea in a cohort of Indian children. PLoS One 6:e28647.
16. Kumthip K, Khamrin P, Ushijima H, Maneekarn N. 2018. Molecular epidemiology of classic, MLB and VA astroviruses isolated from <5year-old children with gastroenteritis in Thailand, 2011-2016. Infect Genet Evol 65:373-379.
17. Jacobsen S, Hohne M, Marques AM, Beslmuller K, Bock CT, Niendorf S. 2018. Co-circulation of classic and novel astrovirus strains in patients with acute gastroenteritis in Germany. J Infect 76:457-464.
18. Zaraket H, Abou-El-Hassan H, Kreidieh K, Soudani N, Ali Z, Hammadi M, Reslan L, Ghanem S, Hajar F, Inati A, Rajab M, Fakhouri H, Ghanem B, Baasiri G, Melhem NM,

Dbaibo G. 2017. Characterization of astrovirus-associated gastroenteritis in hospitalized children under five years of age. Infect Genet Evol 53:94-99.

19. Cordey S, Vu DL, Zanella MC, Turin L, Mamin A, Kaiser L. 2017. Novel and classical human astroviruses in stool and cerebrospinal fluid: comprehensive screening in a tertiary care hospital, Switzerland. Emerg Microbes Infect 6:e84.

20. Khamrin P, Thongprachum A, Okitsu S, Hayakawa S, Maneekarn N, Ushijima H. 2016. Multiple astrovirus MLB1, MLB2, VA2 clades, and classic human astrovirus in children with acute gastroenteritis in Japan. J Med Virol 88:356-360.

21. Xavier Mda P, Carvalho Costa FA, Rocha MS, Andrade Jda S, Diniz FK, Andrade TR, Miagostovich MP, Leite JP, Volotao Ede M. 2015. Surveillance of Human Astrovirus Infection in Brazil: The First Report of MLB1 Astrovirus. PloS One 10:e0135687.

22. Quan PL, Wagner TA, Briese T, Torgerson TR, Hornig M, Tashmukhamedova A, Firth C, Palacios G, Baisre-De-Leon A, Paddock CD, Hutchison SK, Egholm M, Zaki SR, Goldman JE, Ochs HD, Lipkin WI. 2010. Astrovirus encephalitis in boy with X-linked agammaglobulinemia. Emerg Infect Dis 16:918-925.

23. Brown JR, Morfopoulou S, Hubb J, Emmett WA, Ip W, Shah D, Brooks T, Paine SM, Anderson G, Virasami A, Tong CY, Clark DA, Plagnol V, Jacques TS, Qasim W, Hubank M, Breuer J. 2015. Astrovirus VA1/HMO-C: an increasingly recognized neurotropic pathogen in immunocompromised patients. Clin Infect Dis 60:881-888.

24. Naccache SN, Peggs KS, Mattes FM, Phadke R, Garson JA, Grant P, Samayoa E, Federman S, Miller S, Lunn MP, Gant V, Chiu CY. 2015. Diagnosis of neuroinvasive astrovirus infection in an immunocompromised adult with encephalitis by unbiased next-generation sequencing. Clin Infect Dis 60:919-923.

25. Fremond ML, Perot P, Muth E, Cros G, Dumarest M, Mahlaoui N, Seilhean D, Desguerre I, Hebert C, Corre-Catelin N, Neven B, Lecuit M, Blanche S, Picard C, Eloit M. 2015. Next-Generation Sequencing for Diagnosis and Tailored Therapy: A Case Report of Astrovirus-Associated Progressive Encephalitis. J Pediatric Infect Dis Soc 4:e53-7.

26. Lum SH, Turner A, Guiver M, Bonney D, Martland T, Davies E, Newbould M, Brown J, Morfopoulou S, Breuer J, Wynn R. 2016. An emerging opportunistic infection: fatal astrovirus (VA1/HMO-C) encephalitis in a pediatric stem cell transplant recipient. Transpl Infect Dis 18(6):960-964.

27. Sato M, Kuroda M, Kasai M, Matsui H, Fukuyama T, Katano H, Tanaka-Taya K. 2016. Acute encephalopathy in an immunocompromised boy with astrovirus-MLB1 infection detected by next generation sequencing. J Clin Virol 78:66-70.

28. Cordey S, Vu DL, Schibler M, L'Huillier AG, Brito F, Docquier M, Posfay-Barbe KM, Petty TJ, Turin L, Zdobnov EM, Kaiser L. 2016. Astrovirus MLB2, a New Gastroenteric Virus Associated with Meningitis and Disseminated Infection. Emerg Infect Dis 22:846-53.

29. Vu DL, Bosch A, Pinto RM, Guix S. 2017. Epidemiology of Classic and Novel Human Astrovirus: Gastroenteritis and Beyond. Viruses 9.

30. Reuter G, Pankovics P, Boros A. 2018. Nonsuppurative (Aseptic) Meningoencephalomyelitis Associated with Neurovirulent Astrovirus Infections in Humans and Animals. Clin Microbiol Rev 31.

31. Lin HC, Kao CL, Chang LY, Hsieh YC, Shao PL, Lee PI, Lu CY, Lee CY, Huang LM. 2008. Astrovirus gastroenteritis in children in Taipei. J Formos Med Assoc 107:295-303.

32. Tseng WC, Wu FT, Hsiung CA, Chang WC, Wu HS, Wu CY, Lin JS, Yang SC, Hwang KP, Huang YC. 2012. Astrovirus gastroenteritis in hospitalized children of less than 5 years of age in Taiwan, 2009. J Microbiol Immunol Infect 45:311-317.

33. Amaral MS, Estevam GK, Penatti M, Lafontaine R, Lima IC, Spada PK, Gabbay YB, Matos NB. 2015. The prevalence of norovirus, astrovirus and adenovirus infections among hospitalised children with acute gastroenteritis in Porto Velho, state of Rondonia, western Brazilian Amazon. Memorias do Instituto Oswaldo Cruz 110:215-21.

34. Ueda Y, Nakaya S, Takagi M, Ushijima H. 1996. [Diagnosis and clinical manifestations of diarrheal virus infections in Maizuru area from 1991 to 1994--especially focused on small round structured viruses]. Kansenshogaku Zasshi 70:1092-1097.
35. Cordey S, Zanella MC, Wagner N, Turin L, Kaiser L. 2018. Novel human astroviruses in pediatric respiratory samples: A one-year survey in a Swiss tertiary-care hospital. J Med Virol 90:1775-1778.
36. Padmanabhan A, Hause BM. 2016. Detection and characterization of a novel genotype of porcine astrovirus 4 from nasal swabs from pigs with acute respiratory disease. Arch Virol 161:2575-2579.
37. Ng TF, Kondov NO, Deng X, Van Eenennaam A, Neibergs HL, Delwart E. 2015. A metagenomics and case-control study to identify viruses associated with bovine respiratory disease. J Virol 89:5340-5349.
38. Wylie KM, Mihindukulasuriya KA, Sodergren E, Weinstock GM, Storch GA. 2012. Sequence analysis of the human virome in febrile and afebrile children. PloS One 7:e27735.
39. Cordey S, Hartley MA, Keitel K, Laubscher F, Brito F, Junier T, Kagoro F, Samaka J, Masimba J, Said Z, Temba H, Mlaganile T, Docquier M, Fellay J, Kaiser L, D'Acremont V. 2018. Detection of novel astroviruses MLB1 and MLB2 in the sera of febrile Tanzanian children. Emerg Microbes Infect 7:27.
40. Gonzales-Gustavson E, Timoneda N, Fernandez-Cassi X, Caballero A, Abril JF, Buti M, Rodriguez-Frias F, Girones R. 2017. Identification of sapovirus GV.2, astrovirus VA3 and novel anelloviruses in serum from patients with acute hepatitis of unknown aetiology. PloS One 12:e0185911.
41. Gough RE, Collins MS, Borland E, Keymer LF. 1984. Astrovirus-like particles associated with hepatitis in ducklings. Vet Rec 114:279.
42. Zhang Q, Cao Y, Wang J, Fu G, Sun M, Zhang L, Meng L, Cui G, Huang Y, Hu X, Su J. 2018. Isolation and characterization of an astrovirus causing fatal visceral gout in domestic goslings. Emerg Microbes Infect 7:71.
43. Karlsson EA, Small CT, Freiden P, Feeroz MM, Matsen FAt, San S, Hasan MK, Wang D, Jones-Engel L, Schultz-Cherry S. 2015. Non-Human Primates Harbor Diverse Mammalian and Avian Astroviruses Including Those Associated with Human Infections. PLoS Pathog 11:e1005225.
44. Boujon CL, Koch MC, Wuthrich D, Werder S, Jakupovic D, Bruggmann R, Seuberlich T. 2017. Indication of Cross-Species Transmission of Astrovirus Associated with Encephalitis in Sheep and Cattle. Emerg Infect Dis 23:1604-1608.
45. Janowski AB, Bauer IK, Holtz LR, Wang D. 2017. Propagation of astrovirus VA1, a neurotropic human astrovirus, in cell culture. J Virol 91(19).
46. Blight KJ, McKeating JA, Rice CM. 2002. Highly permissive cell lines for subgenomic and genomic hepatitis C virus RNA replication. J Virol 76:13001-13014.
47. Sumpter R, Jr., Loo YM, Foy E, Li K, Yoneyama M, Fujita T, Lemon SM, Gale M, Jr. 2005. Regulating intracellular antiviral defense and permissiveness to hepatitis C virus RNA replication through a cellular RNA helicase, RIG-I. J Virol 79:2689-2699.
48. Koshikawa N, Hasegawa S, Nagashima Y, Mitsuhashi K, Tsubota Y, Miyata S, Miyagi Y, Yasumitsu H, Miyazaki K. 1998. Expression of trypsin by epithelial cells of various tissues, leukocytes, and neurons in human and mouse. Am J Pathol 153:937-944.
49. Boros A, Albert M, Pankovics P, Biro H, Pesavento PA, Phan TG, Delwart E, Reuter G. 2017. Outbreaks of Neuroinvasive Astrovirus Associated with Encephalomyelitis, Weakness, and Paralysis among Weaned Pigs, Hungary. Emerg Infect Dis 23:1982-1993.
50. Brinker JP, Blacklow NR, Herrmann JE. 2000. Human astrovirus isolation and propagation in multiple cell lines. Arch Virol 145:1847-56.

686 51. Oldstone MB. 2006. Viral persistence: parameters, mechanisms and future predictions.
687 Virology 344:111-118.
688 52. Randall RE, Griffin DE. 2017. Within host RNA virus persistence: mechanisms and
689 consequences. Curr Opin Virol 23:35-42.
690 53. Boldogh I AT, Porter DD. 1996. Persistent Viral Infections. *In* S B (ed), Medical
691 Microbiolgy, 4th ed. Galveston (TX):, University of Texas Medical Branch at Galveston; .
692 54. Pinkert S, Klingel K, Lindig V, Dorner A, Zeichhardt H, Spiller OB, Fechner H. 2011.
693 Virus-host coevolution in a persistently coxsackievirus B3-infected cardiomyocyte cell
694 line. J Virol 85:13409-13419.
695 55. Alidjinou EK, Engelmann I, Bossu J, Villenet C, Figeac M, Romond MB, Sane F, Hober D.
696 2017. Persistence of Coxsackievirus B4 in pancreatic ductal-like cells results in cellular
697 and viral changes. Virulence 8:1229-1244.
698 56. Guix S, Perez-Bosque A, Miro L, Moreto M, Bosch A, Pinto RM. 2015. Type I interferon
699 response is delayed in human astrovirus infections. PloS One 10:e0123087.
700 57. Marvin SA, Huerta CT, Sharp B, Freiden P, Cline TD, Schultz-Cherry S. 2016. Type I
701 Interferon Response Limits Astrovirus Replication and Protects against Increased
702 Barrier Permeability In Vitro and In Vivo. J Virol 90:1988-1996.
703 58. Nice TJ, Baldridge MT, McCune BT, Norman JM, Lazear HM, Artyomov M, Diamond MS,
704 Virgin HW. 2015. Interferon-lambda cures persistent murine norovirus infection in the
705 absence of adaptive immunity. Science 347:269-273.
706 59. Lee S, Wilen CB, Orvedahl A, McCune BT, Kim KW, Orchard RC, Peterson ST, Nice TJ,
707 Baldridge MT, Virgin HW. 2017. Norovirus Cell Tropism Is Determined by
708 Combinatorial Action of a Viral Non-structural Protein and Host Cytokine. Cell Host
709 Microbe 22:449-459 e4.
710 60. Konduru K, Kaplan GG. 2006. Stable growth of wild-type hepatitis A virus in cell
711 culture. J Virol 80:1352-1360.
712 61. Jones CT, Catanese MT, Law LM, Khetani SR, Syder AJ, Ploss A, Oh TS, Schoggins JW,
713 MacDonald MR, Bhatia SN, Rice CM. 2010. Real-time imaging of hepatitis C virus
714 infection using a fluorescent cell-based reporter system. Nature Biotechnol 28:167-
715 171.
716 62. Holtz LR, Bauer IK, Jiang H, Belshe R, Freiden P, Schultz-Cherry SL, Wang D. 2014.
717 Seroepidemiology of astrovirus MLB1. Clin Vaccine Immunol 21:908-911.

718

719

720 **Table 1: Summary of the results of HAstV MLB1 and MLB2 propagation on**

721 **selected cell lines**

	HAstV MLB1	HAstV MLB2
Origin of the stool sample	1 year-old child Barcelona, Spain	Adult allogeneic stem cell transplant recipient for acute myeloid leukemia Geneva, Switzerland
Patient's symptoms	Gastroenteritis	Meningo-encephalitis Leukemia relapse
Viral titer of the initial inoculum (genome copies/ml)	$7.9x10^7$	$4.6x10^7$
Acute infections		
Infected cell lines		
▪ CaCo-2 cells	-	ND
▪ HuH-7.5 cells	+	+
▪ HuH-7AI cells	+	+
▪ A549 cells	+	+
Mean viral titers (genome copies/ml of SN)		
▪ HuH-7.5 cells	$4.5x10^6$	$2.8x10^9$
Persistent infections		
Infected cell lines		
▪ CaCo-2 cells	-	ND
▪ HuH-7.5 cells	+	-
▪ HuH-7AI cells	+	+
▪ A549 cells	+	+
Mean viral titers (genome copies/ml of SN)		
▪ HuH-7.5 cells	$5.6x10^9$	-
▪ HuH-7AI cells	$4.3x10^8$	$3.6x10^7$
▪ A549 cells	$4.9x10^8$	$2.5x10^7$
Percentage of infected cells (median)		
▪ HuH-7AI cells	11%	8.8%
▪ A549 cells	4.8%	8.8%

722

723 Mean viral titers for HuH-7AI and A549 cell lines acute infections are not provided due
724 to the few number of assays performed. ND: not done; + successful replication; - failure
725 to replicate.

726

727

728 **Table 2.** Nucleotide **s**equences of the primers pairs used for the sequencing of the whole

729 genomes of HAstV MLB1 and HAstV MLB2 strains recovered from infected cells.

Segment	Primer	MLB1	MLB2
Segment 1	Primer 1 F	CCAAGAGTGGTGGTATGGC	CCAAGAGTGGTGGTATGGC
	Primer 1 R	CAGTGCTGTAGACATCCAGAAA	AGCACAAACAACTGATGTAACT
Segment 2	Primer 2 F	AGAGACCCTGTGTTGCAATAAT	AAAGACCATGTGTTGCCATAAT
	Primer 2 R	CTAACTTTGGCTTGAGCAACATAA	CTAACTTTAGCCTGGGCCACATAA
Segment 3	Primer 3 F	CATAGTTACCGCCGCACAT	TATAGTGACAGCAGCACAT
	Primer 3 R	TTCCCTAGTCAGTCCCTTATCC	TTCTCTGGTTAGGCCTTTATCC
Segment 4	Primer 4 F	CTGACAGAAGAGGAGTACCAAG	TGGCGCACGTCATAGAA
	Primer 4 R	CCCATACAGTGGGACCAAA	CCCATACAGTGGGACCAAA
Segment 5	Primer 5 F	GTACCTTTAGATAGGCCAGTGTATG	GTACCTTTAGATAGGCCAGTGTATG
	Primer 5 R	CATCAACAAGGTTGGTGGTATTG	CACCCATAAGCGAGAACCGTAAT
Segment 6	Primer 6 F	GTTGCGCTCCAAAGGTAATAAA	TCCCTTCTTTGGAGGCTTTG
	Primer 6 R	AGTGAAGCGCCTTGGTAAG	AGTGAAGCGCCTTGGTAAG
Segment 7	Primer 7 F	CCAGTTGTTGATGGCAAATGA	CCAGTTGTTGATGGCAAATGA
	Primer 7 R	CCACTCACTAGACGCTGTTT	TTCACAAGGGCCTGAAAC
Segment 8	Primer 8 F	CTCAACTCATGGTCTGGTCTTG	TTGAATTCATGGTCGGGTC
	Primer 8 R	CATGTGCCTTGCTGGAAATTG	GGTGGGCAGTACTAGAAATTG
Segment 9	Primer 9 F	CAGCGGATGTCTATCGTGTTTA	CAGCTGATGTTTACAGAGTTTACAC
	Primer 9 R	TCCTTAGGTATAGCTGGGTATGT	AATGACCCTGTATGCTGGTATG
Segment 10	Primer 10 F	GGTCATCAGCACCAGCTAATA	GTTCATCTGCAACATCTGAGA
	Primer 10 R	TTTTTTTTTTTTTTTTTTTTTTTTTTTTTTTT TTTTTTTT	TTTTTTTTTTTTTTTTTTTTTTTTTTTTTTTT TTTTTTTTT

730

731

732

733 **Figure legends**

734 **Figure 1. Description of the viral and cell passages performed with HAstV MLB1**
735 **and MLB2 on selected cell lines. (A)** Passage history in HuH-7.5 cells. Initially, cells
736 were infected using clinical stool samples as inoculum. After 7-8 viral passages of
737 HAstV MLB1 and MLB2, respectively, infected cells were subcultured. **(B)** HuH-7AI
738 and A549 cell passages using HuH-7.5 cell lysates as inoculum to establish persistent
739 infections. V-Pn: viral passages; C-Pn: cellular passages; EM: electron microscopy; IF:
740 immunofluorescence; IFN: interferon.

741 **Figure 2. Infection of MLB1 and MLB2 in acutely infected cells. (A)** Viral genome
742 titers detected in the culture supernatant (SN) by RT-qPCR assays. **(B and C)** Electron
743 microscopy of SN from HuH-7.5 cells infected with HAstV MLB1, using SN of a
744 persistently-infected cell line as inoculum **(B)** and MLB2 **(C)**. Bars equal 200 nm.

745 **Figure 3. Multi-step growth curves of MLB1 and MLB2 on HuH-7.5 cells.** Cells
746 were infected using a multiplicity of infection of 20 genome copies/cell, and viral RNA
747 was measured from the cellular **(A)** and supernatant fractions **(B)**. Plot shows average
748 values and error bars indicate one standard deviation from triplicates. **(C) Viral**
749 **replication with or without trypsin for MLB1 and MLB2 on HuH7.5 cells.** Viral
750 replication is expressed as the fold induction of viral genome titers in the SN of infected
751 cells from 1 hpi to 7 dpi. P values comparing fold inductions with and without trypsin
752 for each genotype were not significant (Mann-Whitney test). Plot shows average values
753 and error bars indicate one standard deviation. Samples were quantified in duplicate
754 from one single experiment.

755 **Figure 4. Electron microscopy analysis of the persistent infections on HuH-7.5**
756 **cells. (A)** Non-infected HuH-7.5 cells **(B-F)** and persistently infected HuH-7.5 cells**)**,

showing intracellular capsid arrays of HAstV MLB1, at 4 days post-seeding. Aggregates of astrovirus particles (v) accumulated in the cytoplasm of infected cells around the nuclei (N). Bars equal 5 µm in A and B, 2 µm in C, and 1 µm in D, E and 200 nm in F.

Figure 5. Viral genome titers detected in the culture supernatant (SN) by RT-qPCR assays of MLB1 and MLB2 strains in persistently infected cell lines. (A) Blue line refers to HuH-7.5 cell line, red lines refer to HuH-7AI cell line, green lines refer to A549 cell line and orange line refer to CaCo-2 cell line. Continuous lines with squares refer to HAstV MLB1 strain and dotted lines with triangles refer to HAstV MLB2 strain. The dotted blue line with squares corresponds to the MLB1 persistently-infected HuH-7.5 cell line, using the original stool sample as inoculum. **(B)** Mean viral genome titers of HAstV MLB1 and MLB2 detected by RT-qPCR assays in the SN of persistently infected HuH-7AI and A549 cell lines**.** The average was calculated based on 7-12 numbers, corresponding to the viral genome titers at each cell passage. Error bars indicate one standard deviation. The mean viral titers were significantly different between HAstV MLB1 and HAstV MLB2, when comparing the same infected cell line (*p=0.0009 in HuH-7AI cells, p=0.0018 in A549 cells, Mann-Whitney test).

Figure 6. Immunofluorescence assay of MLB1 and MLB2 persistently infected cell lines. (A) Infected and non-infected (mock) cultures were fixed at confluency and were incubated with primary (anti-MLB1 and anti-MLB2 antibodies, respectively) and secondary antibodies. Green color corresponds to the viral capsid proteins, and blue color to the nuclei. All samples were fixed at 3-5 days post-seeding (magnification, x10-20). **(B)** Estimated proportion of persistently infected cells visualized by the immunofluorescence assay. Central line of each box plot represents the median. Each boxplot includes data from 7-12 fields, from 2 different cell passages. For HAstV

MLB1, the proportion of HuH7-AI infected cells was significantly higher than the proportion of A549 cells (*p=0.0267, Mann-Whitney test). Bars equal 25 µm.

Figure 7. Visualization of capsid arrays by electron microscopy of persistently infected HuH-7AI and A549 cells. (A) Non-infected HuH-7AI cells, **(B)** Non-infected A549 cells, **(C)** HuH-7AI cells persistently-infected with HAstV MLB1, and **(D)** A549 cells persistently-infected with HAstV MLB2. Bars equal 2 µm in main images and 200 nm in enlargements.

Figure 8. IFN-β and IFN-λ1 expression in infected cell lines. (A) Temporal analysis of IFNβ and IFN-λ1 mRNA expression during acute infection in HuH-7 and A549 cells. Cells were infected with a MOI of 1,000 and 20 genome copies/cell for MLB1 and MLB2, respectively, and polyI:C-transfected cells were used as controls. **(B, C)** Immunofluorescence images correspond to an acute infection using the highest MOI possible (25,000 genome copies/cell for MLB1 and 680 genome copies/cell for MLB2**). (D) Analyses of IFN-β and IFN-λ1 expression in persistently-infected cultures.** *Mock* are non-infected cells. *Mock-poly I:C* are non-infected cells transfected with polyI:C (positive control). *Persistent* are persistently-infected cells. *Persistent-polyI:C* are persistently infected cells that were additionally transfected with polyI:C. 1d, 2d, 4d and 7d are the days post-infection (dpi) where IFN expression was measured during acute infections. All samples were quantified at least in duplicate from two distinct experiments.

Figure 9. Effect of exogenous IFN during acute infection (A, B) and in persistently-infected cultures (C-F). Effect of exogenous IFNβ-1a and IFN-λ1 on acutely-infected HuH-7AI and A549 cells by MLB1 **(A)** and MLB2 **(B)**. The graphic illustrates the mean viral titer measured in the supernatant at 4 dpi, and error bars show one standard deviation. There was a statistically significant difference in the viral titer between no

IFN and IFN-β1a and between no IFN and IFN-λ1 (*p<0.01, ** p<0.005, ***p<0.001, ANOVA and Scheffe tests). Effect of exogenous IFN-β1a and IFN-λ1 on HuH-7AI cultures persistently infected with MLB1 **(C)** or MLB2 **(D)**, and on A549 cultures persistently infected with MLB1 **(E)** and MLB2 **(F)**. Data represent the mean±standard deviation titer of viral RNA in the supernatant of each passage measured at 4-6 days post-seeding in the presence or absence of exogenous IFN-β1a or IFN-λ1. All passages were performed in duplicate. P0 corresponds to the viral titer at one day after seeding of the first passage with exogenous IFN. Dotted line indicates the limit of detection. P=passage; SN=supernatant.

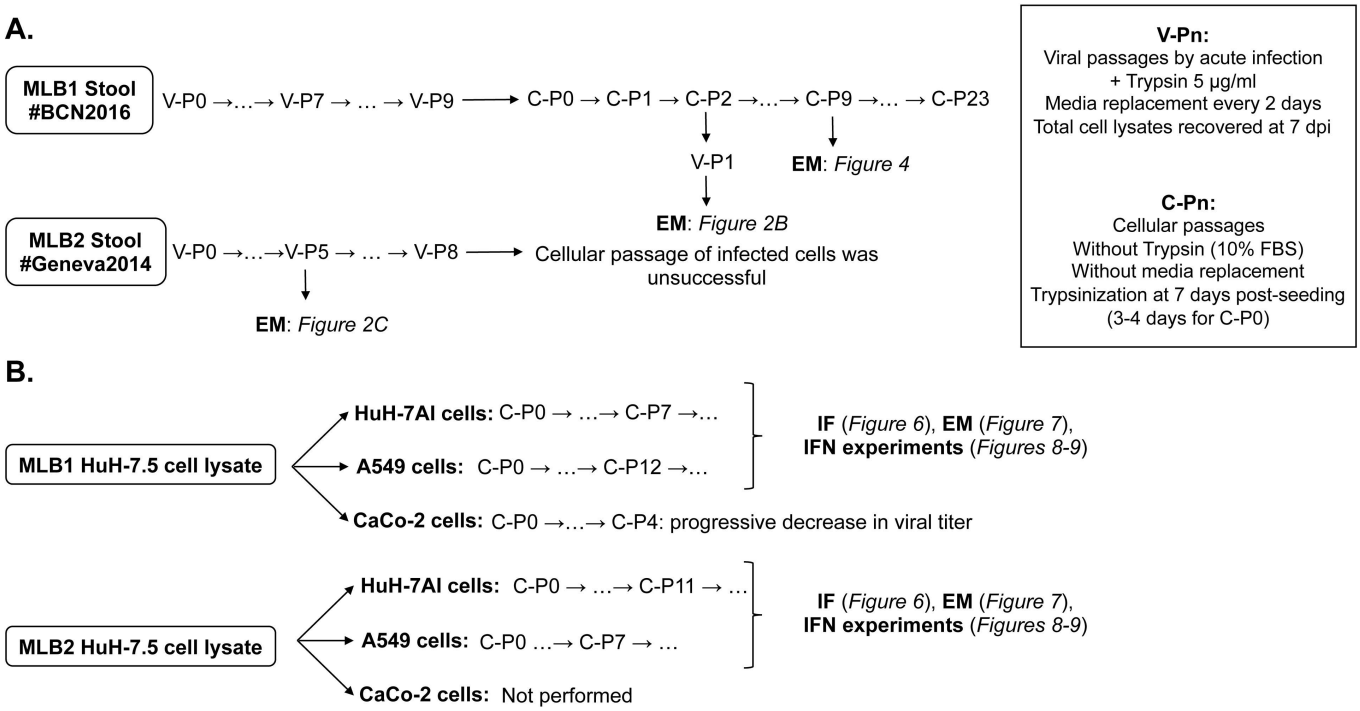

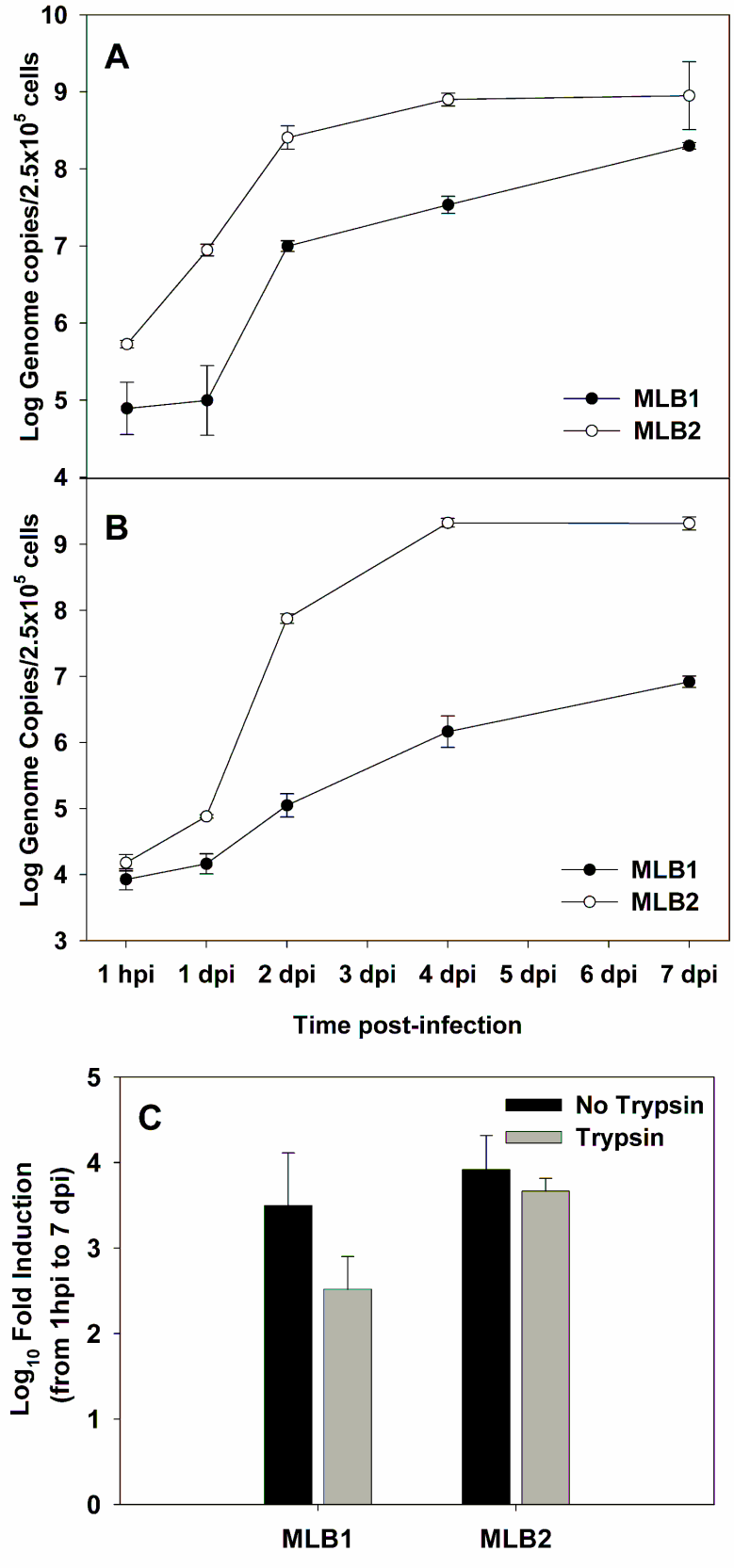

Journal of Virology

JVI

Journal of Virology